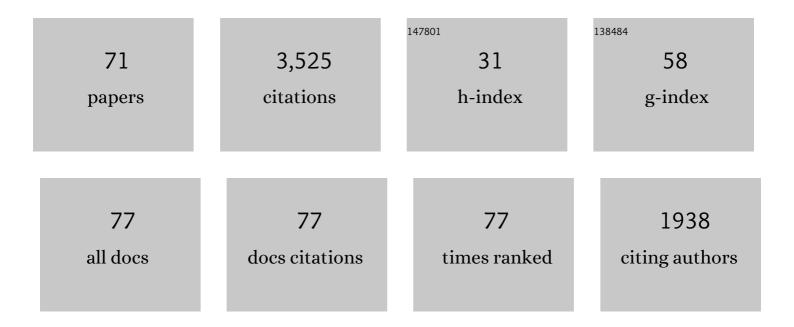
List of Publications by Year in descending order

Source: https://exaly.com/author-pdf/202769/publications.pdf Version: 2024-02-01



#	Article	IF	CITATIONS
1	Ocean acidification and the Permo-Triassic mass extinction. Science, 2015, 348, 229-232.	12.6	284
2	Floral changes across the Triassic/Jurassic boundary linked to flood basalt volcanism. Nature Geoscience, 2009, 2, 589-594.	12.9	227
3	Rapid marine recovery after the end-Permian mass-extinction event in the absence of marine anoxia. Geology, 2004, 32, 805.	4.4	205
4	The lower Triassic anachronistic carbonate facies in space and time. Global and Planetary Change, 2007, 55, 81-89.	3.5	198
5	Multiple episodes of extensive marine anoxia linked to global warming and continental weathering following the latest Permian mass extinction. Science Advances, 2018, 4, e1602921.	10.3	145
6	A unique Permian–Triassic boundary section from the Neotethyan Hawasina Basin, Central Oman Mountains. Palaeogeography, Palaeoclimatology, Palaeoecology, 2003, 191, 329-344.	2.3	127
7	The Global Stratotype Sections and Point (GSSP) for the base of the Jurassic System at Kuhjoch (Karwendel Mountains, Northern Calcareous Alps, Tyrol, Austria). Episodes, 2013, 36, 162-198.	1.2	115
8	Evidence for recurrent changes in Lower Triassic oceanic circulation of the Tethys: The δ13C record from marine sections in Iran. Palaeogeography, Palaeoclimatology, Palaeoecology, 2007, 252, 355-369.	2.3	111
9	Calcimicrobial cap rocks from the basal Triassic units: western Taurus occurrences (SW Turkey). Comptes Rendus - Palevol, 2005, 4, 569-582.	0.2	107
10	Permian–Triassic boundary interval in the Middle East (Iran and N. Oman): Progressive environmental change from detailed carbonate carbon isotope marine curve and sedimentary evolution. Journal of Asian Earth Sciences, 2010, 39, 236-253.	2.3	102
11	Hydrogen sulphide poisoning of shallow seas following the end-Triassic extinction. Nature Geoscience, 2012, 5, 662-667.	12.9	97
12	Microbes, mud and methane: cause and consequence of recurrent <scp>E</scp> arly <scp>J</scp> urassic anoxia following the endâ€ <scp>T</scp> riassic mass extinction. Palaeontology, 2013, 56, 685-709.	2.2	94
13	Dynamic anoxic ferruginous conditions during the end-Permian mass extinction and recovery. Nature Communications, 2016, 7, 12236.	12.8	93
14	Summary of Early Triassic carbon isotope records. Comptes Rendus - Palevol, 2005, 4, 473-486.	0.2	75
15	No causal link between terrestrial ecosystem change and methane release during the end-Triassic mass extinction. Geology, 2012, 40, 531-534.	4.4	70
16	A new high-resolution δ13C record for the Early Triassic: Insights from the Arabian Platform. Gondwana Research, 2013, 24, 233-242.	6.0	69
17	Environmental controls on marine ecosystem recovery following mass extinctions, with an example from the Early Triassic. Earth-Science Reviews, 2015, 149, 108-135.	9.1	69
18	Early Triassic conodonts of Jiarong, Nanpanjiang Basin, southern Guizhou Province, South China. Journal of Asian Earth Sciences, 2015, 105, 104-121.	2.3	63

#	Article	IF	CITATIONS
19	Earliest Triassic microbialites in Çürük Dag, southern Turkey: composition, sequences and controls on formation. Sedimentology, 2011, 58, 739-755.	3.1	61
20	Size variation of conodonts during the Smithian–Spathian (Early Triassic) global warming event. Geology, 2013, 41, 823-826.	4.4	58
21	A review of the evolution, biostratigraphy, provincialism and diversity of <scp>M</scp> iddle and early <scp>L</scp> ate <scp>T</scp> riassic conodonts. Papers in Palaeontology, 2016, 2, 235-263.	1.5	58
22	Sponge-microbial build-ups from the lowermost Triassic Chanakhchi section in southern Armenia: Microfacies and stable carbon isotopes. Palaeogeography, Palaeoclimatology, Palaeoecology, 2018, 490, 653-672.	2.3	55
23	Vertical δ13Corg gradients record changes in planktonic microbial community composition during the end-Permian mass extinction. Palaeogeography, Palaeoclimatology, Palaeoecology, 2014, 396, 119-131.	2.3	52
24	Lower Triassic δ13C isotope curve from shallow-marine carbonates in Japan, Panthalassa realm: Confirmation of the Tethys δ13C curve. Journal of Asian Earth Sciences, 2009, 36, 481-490.	2.3	47
25	The formation of microbial-metazoan bioherms and biostromes following the latest Permian mass extinction. Gondwana Research, 2018, 61, 187-202.	6.0	44
26	Where and when the earliest coccolithophores?. Lethaia, 2012, 45, 507-523.	1.4	43
27	Biogeochemical formation of calyx-shaped carbonate crystal fans in the subsurface of the Early Triassic seafloor. Gondwana Research, 2015, 27, 840-861.	6.0	42
28	The Buday'ah Formation, Sultanate of Oman: A Middle Permian to Early Triassic oceanic record of the Neotethys and the late Induan microsphere bloom. Journal of Asian Earth Sciences, 2012, 43, 130-144.	2.3	39
29	Suppressed competitive exclusion enabled the proliferation of Permian/Triassic boundary microbialites. Depositional Record, 2020, 6, 62-74.	1.7	38
30	A new ostracode fauna from the Permian-Triassic boundary in Turkey (Taurus, Antalya Nappes). Micropaleontology, 2004, 50, 281-295.	1.0	36
31	Early Triassic conodonts and carbonate carbon isotope record of the Idrija–Žiri area, Slovenia. Palaeogeography, Palaeoclimatology, Palaeoecology, 2016, 444, 84-100.	2.3	35
32	The Schandelah Scientific Drilling Project: A 25-million year record of Early Jurassic palaeo-environmental change from northern Germany. Newsletters on Stratigraphy, 2019, 52, 249-296.	1.2	35
33	Global perturbation of the marine calcium cycle during the Permian-Triassic transition. Bulletin of the Geological Society of America, 2018, 130, 1323-1338.	3.3	33
34	Lower Triassic sulphur isotope curve of marine sulphates from the Dolomites, N-Italy. Palaeogeography, Palaeoclimatology, Palaeoecology, 2010, 290, 65-70.	2.3	32
35	Quantitative stratigraphic correlation of Tethyan conodonts across the Smithian-Spathian (Early) Tj ETQq1 1 0.	784314 rgl 9.1	BT /Overlock
36	Geochemistry and mineralogy of the Oligo-Miocene sediments of the Valley of Lakes, Mongolia.	1.5	31

Palaeobiodiversity and Palaeoenvironments, 2017, 97, 233-258.

1.5 $\mathbf{31}$

#	Article	IF	CITATIONS
37	Perturbations in the carbon cycle during the Carnian Humid Episode: carbonate carbon isotope records from southwestern China and northern Oman. Journal of the Geological Society, 2019, 176, 167-177.	2.1	30
38	Evidence for archaeal methanogenesis within veins at the onshore serpentinite-hosted Chimaera seeps, Turkey. Chemical Geology, 2018, 483, 567-580.	3.3	27
39	High-resolution carbon isotope changes, litho- and magnetostratigraphy across Permian-Triassic Boundary sections in the Dolomites, N-Italy. New constraints for global correlation. Palaeogeography, Palaeoclimatology, Palaeoecology, 2010, 290, 58-64.	2.3	26
40	The Sedimentary Geochemistry and Paleoenvironments Project. Geobiology, 2021, 19, 545-556.	2.4	26
41	Multiple sulfur-isotopic evidence for a shallowly stratified ocean following the Triassic-Jurassic boundary mass extinction. Geochimica Et Cosmochimica Acta, 2018, 231, 73-87.	3.9	25
42	"Short" or "long" Rhaetian ? Astronomical calibration of Austrian key sections. Global and Planetary Change, 2020, 192, 103253.	3.5	25
43	Stepwise onset of the Icehouse world and its impact on Oligo-Miocene Central Asian mammals. Scientific Reports, 2016, 6, 36169.	3.3	24
44	Integrated bio-chemostratigraphy of Lower and Middle Triassic marine successions at Spiti in the Indian Himalaya: Implications for the Early Triassic nutrient crisis. Global and Planetary Change, 2021, 196, 103363.	3.5	24
45	Les événements de la limite Permien–Trias : derniers survivants et/ou premiers re-colonisateurs parmi les ostracodes du Taurus (Sud-Ouest de la Turquie). Comptes Rendus - Geoscience, 2002, 334, 489-495.	1.2	22
46	Allometry in <scp>A</scp> nisian (<scp>M</scp> iddle <scp>T</scp> riassic) segminiplanate conodonts and its implications for conodont taxonomy. Palaeontology, 2016, 59, 725-741.	2.2	18
47	Development of early calcareous nannoplankton in the late Triassic (Northern Calcareous Alps,) Tj ETQq1 1 0.78	34314 rgB	Г /Qverlock 1
48	Distribution of iridium and associated geochemistry across the Triassic–Jurassic boundary in sections at Kuhjoch and Kendlbach, Northern Calcareous Alps, Austria. Palaeogeography, Palaeoclimatology, Palaeoecology, 2016, 449, 13-26.	2.3	17
49	New constraints on the evolution of 87Sr/86Sr of seawater during the Upper Triassic. Global and Planetary Change, 2020, 192, 103255.	3.5	17
50	Volcanic temperature changes modulated volatile release and climate fluctuations at the end-Triassic mass extinction. Earth and Planetary Science Letters, 2022, 579, 117364.	4.4	17
51	New hybodontiform and neoselachian sharks from the Lower Triassic of Oman. Journal of Systematic Palaeontology, 2015, 13, 891-917.	1.5	15
52	Western Tethyan Epeiric Ramp Setting in the Early Triassic: An Example from the Central Dinarides (Croatia). Journal of Earth Science (Wuhan, China), 2018, 29, 806-823.	3.2	14
53	Orbital cyclicity in sedimentary sequence and climatic indications of C-O isotopes from Lower Cretaceous in Qingxi Sag, Jiuquan Basin, NW China. Geoscience Frontiers, 2019, 10, 467-479.	8.4	14
54	Smithian and Spathian (Early Triassic) conodonts from Oman and Croatia and their depth habitat revealed. Global and Planetary Change, 2021, 196, 103362.	3.5	14

#	Article	IF	CITATIONS
55	Sponge Takeover from End-Permian Mass Extinction to Early Induan Time: Records in Central Iran Microbial Buildups. Frontiers in Earth Science, 2021, 9, .	1.8	14
56	Permian–Triassic Transition and the Saiq/Mahil Boundary in the Oman Mountains: Proposed correction for lithostratigraphic nomenclature. Geoarabia, 2013, 18, 87-98.	1.6	14
57	Anachronistic facies and carbon isotopes during the end-Permian biocrisis: Evidence from the mid-Tethys (Kisejin, Iran). Palaeogeography, Palaeoclimatology, Palaeoecology, 2019, 516, 364-383.	2.3	12
58	Importance of carbon isotopic data of the Permian-Triassic boundary layers in the Verkhoyansk region for the global correlation of the basal Triassic layer. Doklady Earth Sciences, 2015, 460, 1-5.	0.7	11
59	A new ostracode fauna from the Permian-Triassic boundary in Turkey (Taurus, Antalya Nappes). Micropaleontology, 2004, 50, 281.	1.0	10
60	The dispersal of Halimeda in northern hemisphere mid-latitudes: Palaeobiogeographical insights. Perspectives in Plant Ecology, Evolution and Systematics, 2012, 14, 303-309.	2.7	10
61	Conodont biostratigraphy of the Early Triassic in eastern Slovenia. Paleontological Journal, 2017, 51, 687-703.	0.5	10
62	New data on the structure and age of the terminal Permian strata in the South Verkhoyansk region (<i>northeastern Asia</i>). Russian Geology and Geophysics, 2016, 57, 282-293.	0.7	9
63	The Origin of Carbonate Veins Within the Sedimentary Cover and Igneous Rocks of the Cocos Ridge: Results From IODP Hole U1414A. Geochemistry, Geophysics, Geosystems, 2018, 19, 3721-3738.	2.5	8
64	Middle Triassic conodont assemblages from the Germanic Basin: implications for multi-element taxonomy and biogeography. Journal of Systematic Palaeontology, 2019, 17, 359-377.	1.5	8
65	Palaeo-environmental evolution of Central Asia during the Cenozoic: new insights from the continental sedimentary archive of the Valley of Lakes (Mongolia). Climate of the Past, 2021, 17, 1955-1972.	3.4	8
66	Revised middle Triassic stratigraphy of the Swiss Prealps based on conodonts and correlation to the Briançonnais (Western Alps). Swiss Journal of Geosciences, 2016, 109, 365-377.	1.2	4
67	Early Cambrian brachiopod-dominated shell concentrations from North-East Greenland: Environmental and taphonomic implications. Global and Planetary Change, 2021, 204, 103560.	3.5	3
68	Reply to "Comment on Eoalpine (Cretaceous) evolution of the Oman Tethyan continental margin: insights from a structural field study in Jabal Akhdar (Oman Mountains) by J.P. Breton et al.― (GeoArabia, 2004, v. 9, no. 2, p. 41-58) by D.R. Gray and R.T. Gregory (GeoArabia, 2004, v. 9, no. 4, p. 143-147). Geoarabia, 2005, 10, 203-207.	1.6	3
69	Reply to comments on: A review of the evolution, biostratigraphy, provincialism and diversity of Middle and early Late <scp>T</scp> riassic conodonts. Papers in Palaeontology, 2016, 2, 457-461.	1.5	1
70	Upper Permian to Lower Triassic Carbon Isotope Record in the Oman and Zagros Mountains: An Overview from the Shallow Platform to the Basin. , 2011, , .		0
71	Size Variation of Conodonts During the Smithian–Spathian (Early Triassic) Global Warming Event. Springer Geology, 2014, , 25-27.	0.3	0